Cosmology in the Laboratory: Defect Dynamics in Liquid Crystals
Author(s): Isaac Chuang, Ruth Durrer, Neil Turok and Bernard Yurke
Source: *Science*, New Series, Vol. 251, No. 4999 (Mar. 15, 1991), pp. 1336-1342
Published by: American Association for the Advancement of Science
Stable URL: https://www.jstor.org/stable/2875529
Accessed: 22-07-2019 14:07 UTC

Cosmology in the Laboratory: Defect Dynamics in Liquid Crystals

ISAAC CHUANG, RUTH DURRER, NEIL TUROK, BERNARD YURKE

Liquid crystals are remarkably useful for laboratory exploration of the dynamics of cosmologically relevant defects. They are convenient to work with, they allow the direct study of the "scaling solution" for a network of strings, and they provide a model for the evolution of monopoles and texture. Experiments described here support the simple "one-scale" model for cosmic string evolution, as well as some qualitative predictions of string statistical mechanics. The structure of monopoles and their apparent cylindrical but not spherical symmetry is discussed. A particular kind of defect known as texture is described and is shown to have a dynamical instability—it can decay into a monopole-antimonopole pair. This decay process has been observed occurring in the liquid crystal, and studied with numerical simulations.

A SYMMETRY-BREAKING PHASE TRANSITION IS ONE IN which the symmetry of a system is reduced. The most common example is the freezing of water to ice. In this case, the translational and rotational symmetry of the water is "broken," and the system takes on the discrete symmetry of the ice crystal. As the ice forms, its crystalline orientation varies from one region of space to the next, sometimes producing a mismatch or "defect." The study of the dynamical evolution of such defects produced in symmetry-breaking phase transitions is an increasingly central problem in cosmology, particle physics, and condensed matter physics. The standard model of particle physics and all extensions of it are built on the notion of spontaneously broken internal symmetries. In the standard hot big bang cosmology this automatically leads to defect production as the universe cools through symmetry-breaking phase transitions (*1*). The idea that defects produced in this way later seeded the large-scale structure observed in today's universe has considerable appeal. It is the basis for several models of structure formation: cosmic strings (*2*), textures (*3*), and domain walls (*4, 5*). In particle physics, recent work indicates that processes involving gauged texture in the dynamics of the electroweak phase transition play a major role in determining the final matter-antimatter asymmetry in the universe (*6–9*). In condensed matter physics, attention has increasingly moved to understanding nonequilibrium scaling behavior, particularly near phase transitions (*10–15*).

The universality of symmetry-breaking phenomena suggests that theories dealing with time and space scales beyond the grasp of human manipulation may nevertheless be explored by observing similar systems in which all the relevant lengths have been uniformly scaled down to within reach of the experimentalist, while preserving the essential physics. In this spirit, Zurek proposed (*16*) in 1985 a test of one of the key elements of the cosmological scenario, the Kibble mechanism, through observations of a quench-induced phase transition from normal ^{4}He to the superfluid. His idea was that in a rapid quench, topological string defects (vortex lines) would be created in the same way that some cosmological theories predict. Studying the resulting distribution of strings in the broken symmetry phase might thus give valuable clues about how cosmic strings, the analogous one-dimensional defects in cosmology, should behave. Unfortunately, the experiment was never successfully performed, in part because of the difficulties of working with liquid helium.

The superfluid transition in liquid helium is described in terms of the transition in functional form from a paraboloid to a "Mexican hat" free energy density. The analogy between this and similar "Higgs potentials" in particle physics theories provided the motivation for Zurek's proposal. Such potentials are ubiquitous in particle physics theories, providing the mechanism through which elementary particles get their masses. They are also ubiquitous in the description of phase transitions in condensed matter, so that one might well hope to find a more experimentally tractable physical system in which Zurek's proposal might be realized. Liquid crystals provide such a system.

Liquid crystals (*17–20*) are organic compounds that have phases intermediate to the liquid and solid phases. Most of these mesophases, of which more than eight distinct types have been identified so far, are characterized by certain symmetries in the orientations of the rodlike molecules of the liquid crystalline substances. Typically, phase transitions occur between 10° and 200°C, and result in structures with length scales on the order of tens of micrometers to centimeters which coarsen on experimentally accessible time scales. Their preparation has been extensively studied (*19, 20*) and in contrast to superfluid ^{4}He, they are relatively easy to work with in the laboratory and require only an optical microscope for observation. There is a great body of experimental work on liquid crystals, and several beautiful review articles (*17–23*), some nearly 20 years old. However, the main focus of this work has been on the static properties of defects—we shall be more interested in their dynamics, on which there has apparently been little work.

In this article, we demonstrate that many dynamical phenomena closely analogous to those involved in cosmology and in fundamental particle theories may be directly observed and quantified in a particular liquid crystal, the nematic liquid crystal (NLC). As Zurek originally proposed for ^{4}He, we are able to test the "Kibble mechanism" of defect production in a condensed matter system. Our observations agree well with the ideas of scaling that are central to

I. Chuang and B. Yurke are at AT&T Bell Laboratories, Murray Hill, NJ 07974. R. Durrer and N. Turok are at the Joseph Henry Laboratories, Princeton University, Princeton, NJ 08544.

defect theories of the origin of large-scale structure. Furthermore, we can observe dynamics of the string, monopole, and texture defects found in the NLC. We find the liquid crystal system to be a valuable experimental testing ground for many of the ideas currently being discussed in a cosmological context, and believe that this is an area in which both cosmologists, particle physicists, and condensed matter physicists can benefit from increased interaction.

Topological defects in cosmology. What is a topological defect? In a broken symmetry system, there are many different minimum energy configurations, all related by the underlying symmetry. This set of minimum energy configurations is known as the "vacuum manifold," denoted as $\mathcal{M}_0$. It is the topology of $\mathcal{M}_0$ that determines the existence of defects. The simplest example of this is where $\mathcal{M}_0$ has two disconnected pieces—the system has two distinct minimal energy configurations—as in the Ising model, in which the spins can be either up or down. If a region of "up" spins borders on a region of "down" spins, on the boundary there must be a "wall" of higher energy. This is a "domain wall." Mathematically, one says that the existence of domain walls is guaranteed by the existence of a nontrivial homotopy group, in this case $\pi_0(\mathcal{M}_0)$ corresponding to $\mathcal{M}_0$ being disconnected. Homotopy groups provide a general description of the connectedness properties of spaces: $\pi_0(\mathcal{M}_0)$ gives the number of disconnected pieces of $\mathcal{M}_0$, $\pi_1(\mathcal{M}_0)$ gives the number of topologically distinct noncontractible loops there are on $\mathcal{M}_0$, and in general, $\pi_n(\mathcal{M}_0)$ gives the number of topologically distinct noncontractible n-spheres. Strings occur in theories with nontrivial $\pi_1(\mathcal{M}_0)$. Monopoles occur in theories with nontrivial $\pi_2(\mathcal{M}_0)$ (noncontractible two-spheres in $\mathcal{M}_0$), and textures in theories with nontrivial $\pi_3(\mathcal{M}_0)$ (noncontractible three-spheres in $\mathcal{M}_0$). A further distinction occurs because in particle theories, symmetries are sometimes gauged (that is, involving a gauge field like the vector potential of electromagnetism). This has important consequences for the defect dynamics. We refer to defects produced by gauge-symmetry breaking as being "gauged" defects, and otherwise, as "global" defects (Table 1).

A crucial question for cosmology is the nature of the distribution of the defects produced in symmetry-breaking phase transitions. The picture of defect formation that has been applied in all these cases is called (in particle physics) the "Kibble mechanism." The idea here is that at the time the defects freeze out, there is a characteristic scale ξ beyond which the order parameter (the direction of symmetry breaking) is uncorrelated. To estimate the defect density at formation, one associates a point on $\mathcal{M}_0$ at random to every domain ξ^3, and continues the order parameter from one domain to the next in as smooth a manner as possible. One then forms defects at a density of order one per volume ξ^3. Strings, monopoles, and textures are all formed in the liquid crystal through the Kibble mechanism, and in principle it can be used to calculate the defect density and distribution at the symmetry-breaking phase transition. Knowing the initial distribution and combining this with a model for the evolution of the defect tangle, one may calculate the distribution at later times. It is this which we have tested experimentally.

The evolution of cosmic strings, following their production through the Kibble mechanism, has been extensively investigated numerically and analytically. In particular, this work has led to the development of a simple scaling model for describing the evolution of the string network. At the phase transition, most of the string length is in infinite strings, with the remainder in a scale invariant distribution of loops (*24–27*). Subsequently the string network rapidly enters the "scaling solution," in which it evolves in a self-similar fashion and can at all times be characterised by a single scale. In units of that scale the network looks the same (in a statistical sense) at all times. The scale is both the typical radius of curvature of the strings and their typical separation (*27, 28*).

Table 1. Defects and their role in cosmology.

Defect	Homotopy group	Behavior
Walls	$\pi_0(\mathcal{M}_0)$	Rapidly dominate universe. Disastrous unless formed late.
Strings	$\pi_1(\mathcal{M}_0)$	Global or gauged—scale with density in the universe.
Monopoles	$\pi_2(\mathcal{M}_0)$	Gauged—rapidly dominate universe. Global—scale with density in the universe.
Textures	$\pi_3(\mathcal{M}_0)$	Gauged—relax to vacuum. Global—scale with density in the universe.

For the relativistic strings that occur in cosmology, the scale grows at the speed of light. It is this that enables structures on a scale of megaparsecs to be formed from defects that were originally created when the characteristic scale was microscopic. When the universe becomes dominated by matter rather than radiation, matter perturbations start to grow around the defect "seeds." The (comoving) horizon scale at this time (light travel distance since the big bang) is about 30 Mpc, and this scale is imprinted on the matter distribution, similar to what is seen in large scale galaxy redshift surveys. Unfortunately for strings the characteristic scale on the network is around a tenth of the horizon, and this has led to doubts as to whether strings can produce the observed large-scale structure. Nevertheless, this "one-scale" model developed for understanding cosmic string evolution (*27*) can be directly tested in the liquid crystal system as we shall describe.

Magnetic monopoles have been a long-standing problem for grand unified theories, because any theory starting from a simple gauge group, such as SU(5), and breaking down to electromagnetism at low energies, must produce monopoles. Gauged monopoles annihilate very slowly and come to dominate the universe. Consequently, the simplest combinations of grand unified theories with the standard hot big bang model are ruled out (there are several mechanisms to avoid this problem, one being an epoch of inflation). Global monopoles (*29*), which occur when a global symmetry is broken and $\pi_2(\mathcal{M}_0)$ is nontrivial, evolve quite differently. These enter a scaling solution in a very similar manner to texture (*30, 31*). Global monopoles occur in abundance in the liquid crystal, and are observed to annihilate rapidly in the coarsening of the defect tangle.

Texture is the most recently investigated cosmic defect (*3*). A similar theorem to that involved in the monopole case holds here—whenever a non-Abelian symmetry is broken to an Abelian one, texture is formed. It is therefore very generic and in fact occurs in both parts of the standard model. In the electroweak theory, the vacuum is just a three-sphere and texture plays a central role in processes that violate baryon number conservation, as stated above. Texture also occurs in quantum chromodynamics, where (in the low energy pion dynamics model) the proton itself actually occurs as a π_3 texture (the "Skyrmion"). In this case it is stabilized (by hand) by the addition of higher derivative terms. Without these terms, a texture will collapse and unwind itself (*3*). Our experimental observations and computer simulations confirm this behavior in the nematic liquid crystal.

Global texture, like cosmic strings, also enters a scaling solution. Here the mechanism is simply the redshifting away of energy in Goldstone modes within the horizon, while the fields remain frozen on larger scales. An advantage over strings, as shown by numerical simulations (*32*), is that the characteristic scale for texture is always the horizon scale, so that texture is better at generating large-scale structure than strings. It now appears very promising as a mechanism for generating large-scale structure in the universe—detailed calculations have shown that it correctly predicts the galaxy-galaxy

correlation function, and other cosmic statistics (*33, 34*). It also produces a distinctive pattern of hot and cold spots on the microwave sky at a level which may be detectable soon (*30*).

Topological defects in liquid crystals. Nematic liquid crystals (NLCs) are systems in which the three most interesting cosmic defects—strings, monopoles, and texture—all occur simultaneously. We shall briefly review the mechanics of the NLC, noting the similarities and differences with field theories of cosmological relevance. Following that, we discuss the defect structures which the NLC supports, and finally, we turn to the theory and observation of the dynamics of the defect tangle.

Nematic liquid crystal dynamics. A nematic liquid crystal may be thought of as a fluid made of rodlike molecules. As originally pointed out by Onsager, the nematic-isotropic phase transition is most simply understood as occurring through competition between positional entropy, which favors the rods being randomly located, and orientational entropy, which favors them being randomly oriented. At high concentrations, or low temperatures, maximizing positional entropy is most important, and the favored phase is the "nematic" phase, where the rods are nearly parallel. Conversely, at low concentrations or high temperature, the "isotropic" phase is instead favored. Onsager's simple treatment indicates the transition to be first order, in agreement with experiment; for a critical discussion, see Vertogen and de Jeu (*18*).

The order parameter in the liquid crystal is given by the "director" field $\mathbf{n}$, which is just the local orientation of the rod molecules. By definition, $\mathbf{n}$ has unit length, and is to be identified with $-\mathbf{n}$, because the rods are not directional. The vacuum manifold $\mathcal{M}_0$ is therefore S_2/Z_2, the two-sphere with antipodal points identified. Using an exact homotopy sequence, one can show that the homotopy of $\mathcal{M}_0$ is as follows: $\pi_1(\mathcal{M}_0) = Z_2$, $\pi_2(\mathcal{M}_0) = Z$, $\pi_3(\mathcal{M}_0) = Z$. Thus, we should expect to find one type of string, integrally charged monopoles (*35*), and integrally charged texture. The first two are singular in the sense that at the center of a string or monopole $\mathbf{n}$ changes discontinuously. Texture is completely nonsingular, but cannot exist in a static configuration—it evolves by collapsing and unwinding itself. As it does so it must produce a singular region for an instant. We shall see that in the liquid crystal this happens in an interesting manner.

Because there are no gauge fields in the NLC, the dynamics are most similar to that for a field theory with spontaneously broken global symmetry. The relativistic field theory most analogous to the nematic liquid crystal is one where a global SO(3) internal symmetry (*36*) is spontaneously broken to O(2) by a traceless symmetric tensor Φ_{ab}, $a, b = 1,2,3$. The analogous condition to $|\mathbf{n}|^2 = 1$ is that Φ lie on the minima of a potential $V(\Phi)$ which is invariant under SO(3). For these minima, one can write $\Phi_{ab} = n_a n_b - \frac{1}{3}\delta_{ab}$ with n_a a three-component vector. In the field theory, there are, of course, no singularities—instead ϕ is allowed to vanish at some local cost in potential energy.

The field theory has identical topological properties to the liquid crystal. However, there are two important differences in the dynamics. The most obvious is that dissipation is always important in the liquid crystal, where the defect dynamics are friction dominated. A similar situation occurs in cosmological defects soon after they form, when scattering of particles by the defects is still important.

A more fundamental difference, however, is that whereas the field theory is invariant under global SO(3) rotations in internal space, $\mathbf{n}' = \mathbf{On}$, and spatial rotations $\mathbf{x}' = \tilde{\mathbf{O}}\mathbf{x}$ separately, the liquid crystal is only invariant under the diagonal subgroup of "rigid" rotations, where $\tilde{\mathbf{O}} = \mathbf{O}$. Thus, while the local energy density of a static configuration in the field theory is dictated by symmetry to be:

$$\mathcal{E}_{\text{ft}} = \frac{K}{2}(\nabla_a n_b)^2 \tag{1}$$

the local energy density in the liquid crystal has in general four terms of second order in derivatives:

$$\mathcal{E}_{\text{lc}} = \frac{1}{2}\{K_1(\nabla \cdot \mathbf{n})^2 + K_2(\mathbf{n} \cdot \nabla \times \mathbf{n})^2 + K_3[\mathbf{n} \times (\nabla \times \mathbf{n})]^2 + K_4\nabla \cdot [(\mathbf{n} \cdot \nabla)\mathbf{n} - \mathbf{n}(\nabla \cdot \mathbf{n})]\} \tag{2}$$

Usually, the K_i are not equal; for our particular NLC it has been determined that $K_1 \approx 1.15 \times 10^{-6}$, $K_2 \approx 0.6 \times 10^{-6}$, and $K_3 \approx 1.55 \times 10^{-6}$ dynes at 25°C (*37*). The fourth term is a surface energy and often neglected because it does not show up in the equations of motion. The four terms in Eq. 2 are known as the splay, twist, bend, and saddle-splay curvature terms, respectively (*21*).

Liquid crystals are often discussed in the "one-constant" approximation where $K_1 = K_2 = K_3 \equiv K$ In this case:

$$\mathcal{E}_{\text{lc}} = \mathcal{E}_{\text{ft}} + \frac{K_4 - K}{2}\nabla \cdot [(\mathbf{n} \cdot \nabla)\mathbf{n} - \mathbf{n}(\nabla \cdot \mathbf{n})]$$

so that the two energy functionals are equal up to a surface term. In the one-constant approximation, the equations of motion derived from Eq. 2 possess the full internal and spatial rotational symmetries. Thus, after the phase transition we should find that all defects related by internal rotations occur with exactly equal abundances in the bulk. If we use a local energy functional to decide which defects are lower energy and thus more numerous, we must use an expression that respects this symmetry, and therefore set $K_4 = K$ in Eq. 2. In the unequal constant case we have no similar guiding principle, and K_4 must be determined by other means. This is important for monopoles, where the surface term scales as area $\times$ $r^{-1} \propto r$, like the total monopole energy, but is apparently ignored in (*17*).

In the unequal constant case, configurations that differ by an internal rotation, $\mathbf{n}' = \mathbf{On}$, in general also differ in energy. Finding analytical solutions that minimize Eq. 2 is in most cases very difficult, but a perturbative analysis, where the K_i are nearly equal, is straightforward and illustrates some important effects. One finds in particular that up to "rigid" rotations, and some discrete degeneracies, the rod orientations in the minimal energy configurations are completely fixed.

Monopoles and strings in the NLC. The general one-constant monopole is written as $\mathbf{n} = \mathbf{Ox}/r$, that is, a global rotation of the "hedgehog" monopole (it is called a hedgehog monopole because all of the molecules are oriented radially out from the center of the defect). The structure of the minimal energy monopole in the unequal constant case can be calculated by minimizing the energy perturbation with respect to O. In the case where $\delta K_1 = \delta K_3 > 0$, $\delta K_2 = 0$, with "free" boundary conditions (*38*) we find that the minimal energy monopole is given (up to rigid rotations) by $\mathbf{n} = \hat{\mathbf{x}}$ $\sin\theta\cos(\phi - 2\pi/3) + \hat{\mathbf{y}}\sin\theta\sin(\phi - 2\pi/3) + \hat{\mathbf{z}}\cos\theta$ with θ, ϕ the usual polar angles. As long as the δK_i are different, the minimal energy solution is cylindrically rather than spherically symmetric.

Recently Goldhaber pointed out that monopoles in the one-constant approximation actually have an even larger degeneracy in energy (*39*). He showed that there is a class of deformations that, at no cost in energy, concentrate all of the "flux" from a monopole into a single arbitrarily thin tube. If this were true in our system, one might expect to see some monopoles at the "ends" of flux tubes (*40*). Instead, in the monopoles we observe experimentally, the flux appears to emerge in two opposing tubes, in an apparently stable configuration. It is a simple but lengthy calculation to apply Goldhaber's deformation to the $\delta K_1 = \delta K_3 > 0$, $\delta K_2 = 0$ monopole above, and calculate the dependence of the energy perturbation on the deformation parameter. We have done this and find that it is

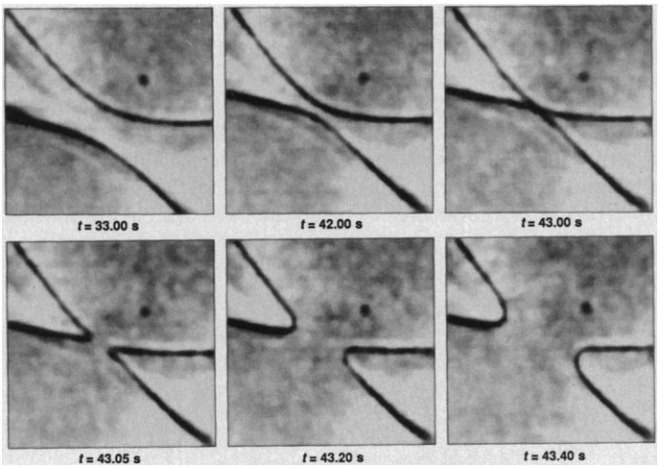

Fig. 1. String intercommutation sequence, showing two type-$\frac{1}{2}$ strings crossing each other and reconnecting the other way. Each picture shows a region 140 μm in width. Note that the two strings lie almost in the same plane—the intercommutation occurs after the strings move toward each other under their mutual attraction.

stable. Thus, monopoles survive in cylindrically symmetric, stable configurations.

We now turn to strings. These are related to noncontractible loops on $\mathcal{M}_0$—as one encircles a string in space the director $\mathbf{n}$ rotates around to $-\mathbf{n}$. Again in the field theory, all great semicircle paths along $\mathcal{M}_0$ are degenerate in energy, and one would expect to find all of the corresponding strings with equal probability. However, with unequal constants the degeneracy is broken. Just as in the monopole case, we write the family of degenerate unperturbed solutions as $\mathrm{O}\mathbf{n}_p$ with O, a constant rotation matrix and the "planar" solution $\mathbf{n}_p = \hat{\mathbf{x}} \cos(\phi/2) + \hat{\mathbf{y}} \sin(\phi/2)$ with ϕ the azimuthal angle. In this case, up to rigid rotations about the z-axis, one finds the minimal energy solutions are given (for $\delta K_1 = \delta K_3 > 0$, $\delta K_2 = 0$) by $\mathbf{n} = \hat{\mathbf{x}} \cos(\phi/2) \pm \hat{\mathbf{z}} \sin(\phi/2)$—the director twists out of the plane perpendicular to the string as one moves around it.

Instead of an infinite set of string solutions we are left with just two—a "$+\frac{1}{2}$" string and a "$-\frac{1}{2}$" string. These are topologically equivalent, but separated by an energy barrier in the unequal constant case. It is not hard to see that a loop of $+\frac{1}{2}$ string actually carries monopole charge unity, so as $+\frac{1}{2}$ loops shrink they should produce a monopole. We have observed this to happen only rarely—more often, they shrink and disappear without trace. A possible explanation for this is as follows. Loops are created by a long string intersecting itself. However a $\pm\frac{1}{2}$ string repels itself (*19*), and therefore pure $+\frac{1}{2}$ loops would only rarely be chopped off from long strings. However, if a long string contains a "junction" between a $+\frac{1}{2}$ and a $-\frac{1}{2}$ string, the two parts attract, and are more likely to intersect and chop off a loop. This would then be comprised of a section of $+\frac{1}{2}$ joined to another of $-\frac{1}{2}$ string. Such a loop can collapse without leaving a monopole.

One question of considerable importance to cosmic strings is the question of what happens when two strings cross. We frequently observe "intercommutation," that is, two strings reconnecting the other way as they cross. An example is shown in Fig. 1. This process has been simulated numerically by many people in particle physics (*41, 42*) and condensed-matter physics (*43, 44*), but has eluded documentation in a laboratory system. Intercommutation also sometimes results in a ±1 string (below) connecting the two reconnection points.

If two parallel $+\frac{1}{2}$ strings combine, a "+1 string" results. As one encircles a +1 string, $\mathbf{n}$ follows an entire great circle around the sphere. The +1 and −1 strings are topologically trivial, because the paths followed by $\mathbf{n}$ can be continuously contracted to a point—either to one side or the other of the great circle. This is colloquially referred to as the rods "escaping in the third dimension" (*40, 45*). By escaping, the NLC avoids the logarithmic divergence in energy at the core of a singular string. Thus ±1 strings are more like "flux tubes" than strings; evidently, there are nothing but boundary conditions to prevent ±1 strings from spreading out in all of space. In fact, it is something of a puzzle that they appear to have as definite a width as they do. Monopoles emit two ±1 strings opposite each other, which are in some cases quite constant in width for large distances—a sort of "flux confinement." Energetics, however, favor the ±1 strings spreading out; the energy of a monopole with "unconfined" flux scales as R, the size of the region enclosing it, but the energy of a flux tube scales as $R \ln(R/r_c)$ where r_c is the core radius. For large R the monopole field must spread out. The apparent "flux confinement" seems to conflict with this simple argument, and bears further investigation. Ignoring this, if one calculates perturbatively as above, the minimal energy ±1 string is given (outside the core, for $\delta K_1 = \delta K_3 > 0$, $\delta K_2 = 0$) by $\mathbf{n} = \hat{\mathbf{x}} \cos\phi \pm \hat{\mathbf{y}} \sin\phi$).

To summarize, in the liquid crystal the infinite degeneracy between defects related by internal rotations is broken to a discrete one. For monopoles there is a single minimal energy configuration, for $\frac{1}{2}$ strings there are two ($\pm\frac{1}{2}$), and for flux tubes four (±1 tubes "escaped" in either direction). Shown in Fig. 2 are a plethora of defects, typical of what we see after a thermal quench.

Experimental observations: Texture decay and scaling exponents. We have constructed an apparatus for studying rapid pressure and temperature induced isotropic-nematic transitions in a nematic liquid crystal, 4-cyano-4′-*n*-pentylbiphenyl (commercially known as K15, or 5CB). This NLC has an isotropic to nematic transition temperature at 35.3°C, and a nematic to crystalline transition at 24°C. In a rapid isotropic to nematic transition, strings, monopoles, and textures are produced. We have methodically studied the

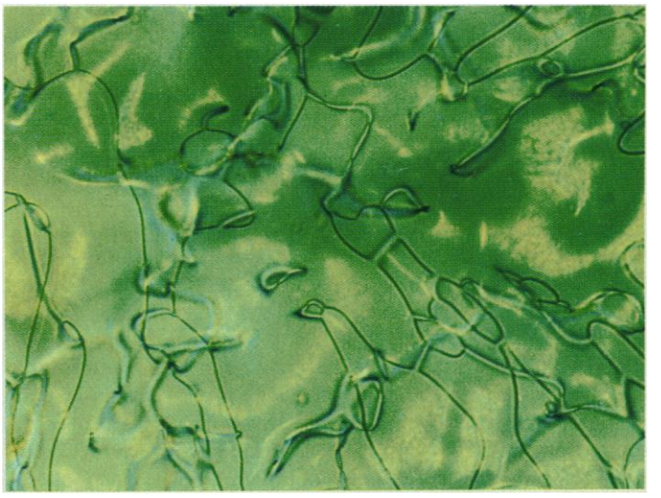

Fig. 2. A picture of the defect tangle in a thin film of freely suspended nematic liquid crystal after a temperature quench. The dark, sharp lines in the picture are type-$\frac{1}{2}$ strings. In the top-center of the picture is a diffuse but visible type-1 string with three monopoles, which appear as black spots on the string. Below that is a type-$\frac{1}{2}$ string attached in two places to a type-1 string which is also supporting a monopole. Various other features in the photograph include boojums, which are defects which are attached to the surface of the film (*37*) and appear as lines which terminate in dark blobs, and many instances of type-1 strings cutting across horseshoe-shaped type-$\frac{1}{2}$ strings. The picture shows a region 790 μm in width.

evolution of strings and monopoles in a pressure cell photographically and with a high-speed video system, and we have also attempted to create textures in a freely suspended thin film of the NLC, using a hand-controlled probe. Our observations of texture decay and our string density scaling data are in agreement with theoretical predictions.

Texture decay in the NLC. Our first question in seeking a texture experimentally is, what does it look like? Texture is hard to visualize as it is not localized and may only develop a singularity for an instant as it unwinds itself. Mathematically, texture corresponds to homotopically nontrivial maps from S_3 (space with infinity identified) to S_2. These maps are a special case of the Hopf fibration (*46*), and may be constructed from applying local rotations to a uniform director field as follows. We use the fact that the group SU(2) is, as a topological space, a three sphere. A map from physical space onto SU(2) with winding number one is provided by $g(\mathbf{x}) = \exp(i\chi(r)\mathbf{x}\cdot\boldsymbol{\sigma}/r)$ with the Pauli matrices $\boldsymbol{\sigma}$ and $\chi(r)$ (a polar angle on the three sphere) a function running from 0 at the origin to π at infinity. Now, to map this onto S_2, we simply use $\mathbf{n}(\mathbf{x})\cdot\boldsymbol{\sigma} = g(\mathbf{x})\sigma_3 g(\mathbf{x})^{-1}$. The resulting director field is:

$$\mathbf{n} = \left[\frac{2xz}{r}\sin^2\chi - y\sin 2\chi\right]\frac{\hat{\mathbf{x}}}{r} + \left[\frac{2yz}{r}\sin^2\chi + x\sin 2\chi\right]\frac{\hat{\mathbf{y}}}{r} + \left[\frac{2z^2}{r^2}\sin^2\chi + \cos 2\chi\right]\hat{\mathbf{z}} \quad (3)$$

The energy density of this configuration is concentrated in a ring around the z-axis, lying in the $x - y$ plane. The configuration is actually equivalent to a $+1$ ring (which carries two units of monopole charge) surrounded by a -1 ring (which cancels the monopole charge). There are no singularities anywhere, but by Derrick's theorem (*47*), the configuration must collapse and unwind itself, or be stabilized by higher derivative terms. This latter possibility was considered by Wu and Zee (*48*). Because we do not see stable textures experimentally in the NLC, we assume that the latter possibility is not realized. To see that the configuration is topologically nontrivial, and must produce a singularity in the unwinding process, consider lines of constant $\mathbf{n}$ in space. These lines form two rings about the z-axis that link once. If the configuration is to relax to a configuration of constant $\mathbf{n}$, these linked lines must cross. It being impossible for $\mathbf{n}$ to take two values at once, there must be a singularity produced at the crossing point (*21, 22*).

We have not seen objects like this produced in pressure jumps or temperature quenches, and so are faced with the question: why is texture so rare? To answer this, we performed a simple relaxation simulation of a liquid crystal in the one-constant approximation. Space is discretized as a cubic (40^3) lattice, and multiple sweeps through the lattice are performed, minimizing the energy at each site as a function of the director at that site while keeping the director at neighboring sites fixed. The initial shape and size of the texture is fixed by $\chi(r) = \pi\{1 + \tanh[(r - S)/W]\}$, where S determines the size of the ring and W its width. A perfectly circular texture of this form collapses to a point and unwinds itself. However, if slightly perturbed, replacing the argument of the hyperbolic tangent by $[r - S(1 + \frac{1}{2}\cos\phi)]/W$, with ϕ the azimuthal angle, a very different evolution is observed. Instead of a uniform shrinking, the ring pinches off at one point, forming a monopole-antimonopole pair, clearly visible in plots of the director field. The monopoles then travel around opposite halves of the ring and annihilate on the far side. This simulation provides a possible answer to our question. Texture has a decay channel into monopole-antimonopole pairs. In terms of the linked lines of the previous paragraph, it is evident that the monopole and antimonopole act as sources from which all lines emerge. The linked lines evidently all cross at once, forming the pair, and then break apart as the monopole-antimonopole pair move apart.

In order to observe this decay mode in the NLC, we manipulated a freely suspended thin film of NLC with a glass whisker probe, mounted on a micrometer stage, in an attempt to hand-manufacture a texture defect. We found that linear motion of the probe through the crystal readily produced ± 1 defect lines and that circular motion

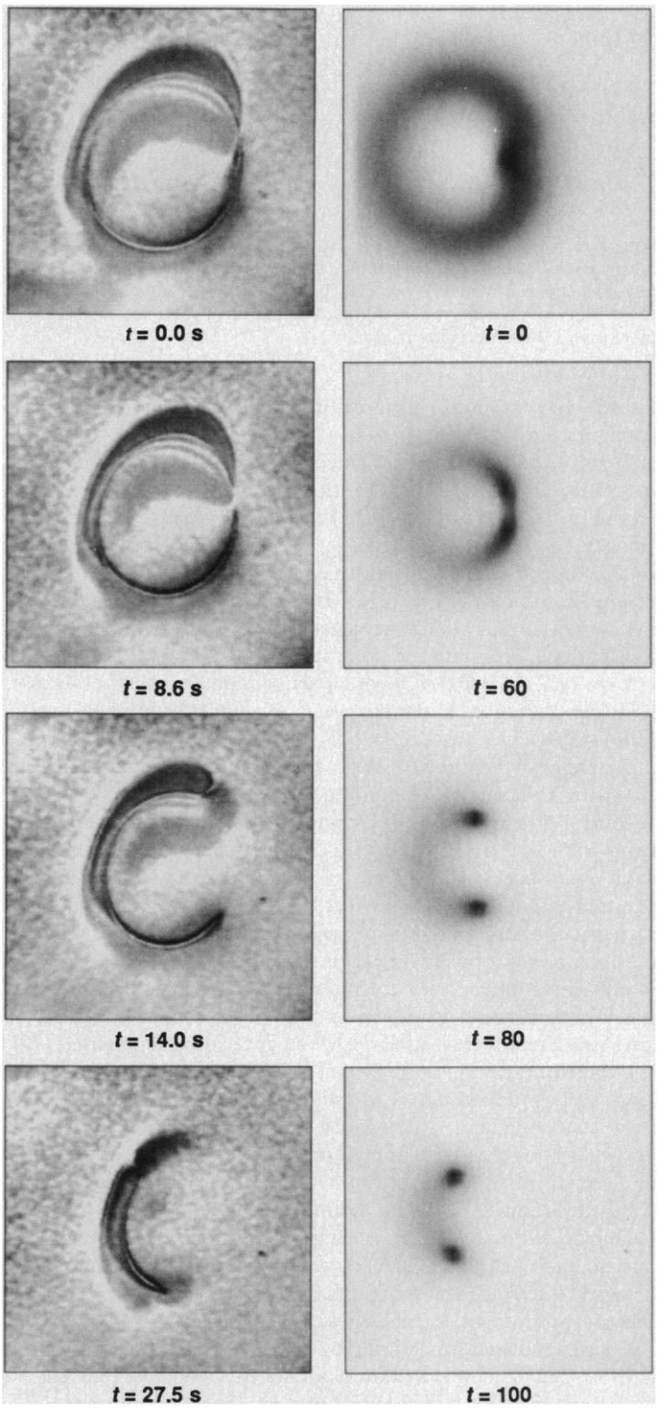

Fig. 3. A time sequence showing the evolution of a π_3 "texture" in a freely suspended thin film of nematic liquid crystal (left column) and as simulated numerically (right column). The texture breaks at one point to form a monopole-antimonopole pair, which then moves around the ring to annihilate on the far side. Each frame shows a region 260 μm in width.

sometimes produced ±1 rings which had no monopoles attached to them. Because the ±1 rings we observed were able to unwind without leaving any remnants, we inferred that each ±1 ring must have been surrounded by a diffuse ∓1 ring, in order to cancel the topological charge. We then observed several rings break apart at one point, producing a monopole-antimonopole pair in the same manner as the computer simulations did. A sequence of four pictures taken from the microscope demonstrating this evolution are shown alongside four simulation-generated pictures in Fig. 3 (in which $S = 10$ and $W = 6$). Note the more distinct "flux tubes" in the liquid crystal, in line with our discussion above. We conclude that this decay channel is real and is the likely explanation for the apparent absence of texture in the NLC.

Scaling dynamics in the nematic liquid crystal. Finally, we consider the coarsening dynamics of the defect tangle, after a rapid phase transition. We are primarily concerned with understanding the evolution of the string density. The singular $\pm\frac{1}{2}$ strings have higher tension and thus presumably dominate the dynamics, so to a first approximation we shall only consider their interactions. According to the "one-scale" model for a network of long strings, it should at all times be characterized by a single scale ξ. This may be defined in terms of the long string density: $\rho \equiv 1/\xi^2$ is the length of string per unit volume. The postulate is that at all times ξ is both the typical radius of curvature on the strings and the typical string-string separation. There are two important processes to consider.

First, there is the effect of viscous drag. Let the string tension be T, and the frictional force per unit length be Γv, with v the velocity. Balancing the tension force of T/ξ per unit length against the drag, we find that a segment of string of radius of curvature ξ reaches a terminal velocity $v = T/\Gamma\xi$. The rate of loss of energy from the string is approximately $\dot{W} = Tv\rho/\xi = T^2\rho^2/\Gamma$ per unit volume, and the rate of decrease of ρ can be calculated by equating this energy loss with the time derivative of the equilibrium string energy density $W = T\rho$. Assuming T to be a constant (*49*) we get:

$$\frac{d\rho}{dt} = -c\frac{T}{\Gamma}\rho^2 \qquad (4)$$

where a constant of proportionality, c, has been introduced.

Second, we should include the loss of length from the long strings into loops: this is always favored by phase space over reconnection of loops onto long string (*27*). A long string loses length to loops at a rate given by a geometrical constant times v/ξ, which scales the same way as the viscous force damping term. Thus, the constant c may be taken to include both these effects. Inserting the definition of ρ in Eq. 4 we find that the scaling solution is given by $\rho = (\Gamma/cT)t^{-1}$.

We should note that similar arguments have also been given in the condensed matter literature before—applied both to domains in two dimensions (*50*) and strings in three (*13*). In two dimensions one obtains for the string length per unit area $\rho = 1/\xi \propto t^{-1/2}$. With the assumption of scaling, the derivation of the exponent is little more than dimensional analysis. However, this basic assumption seems to have been studied and tested more comprehensively in the cosmological literature (*27, 51, 52*) for string networks at least.

The two-dimensional scaling has been experimentally investigated by Orihara, Ishibashi, and Nagaya (*53, 54*). We have experimentally tested the $\rho \propto t^{-1}$ string density scaling prediction in three dimensions by recording high-speed video pictures of the string network which forms after performing a rapid pressure jump (of ΔP) to force an isotropic to nematic phase transition. The data are analyzed by digitizing selected pictures and by locating the strings with a gradient-seeking algorithm. Four typical pictures of the string tangle in evolution are shown in Fig. 4. For times between 1 second and 32 seconds, the string network was both low enough in density for the strings to be clearly distinguished and high enough in density that finite size effects were negligible. The results, shown in Fig. 5, fit the predicted t^{-1} power law remarkably well. Repeating the experiment at increasing ΔP, we found the same scaling with time, but decreasing string density at a fixed time, consistent with the effect expected above, where if the string tension is increased, so is the scaling value of ξ.

Future directions. In this article, we have made considerable progress in the study of the dynamical evolution of topological defects in liquid crystals. Our results include simulation and observation of texture decay through monopole-antimonopole creation,

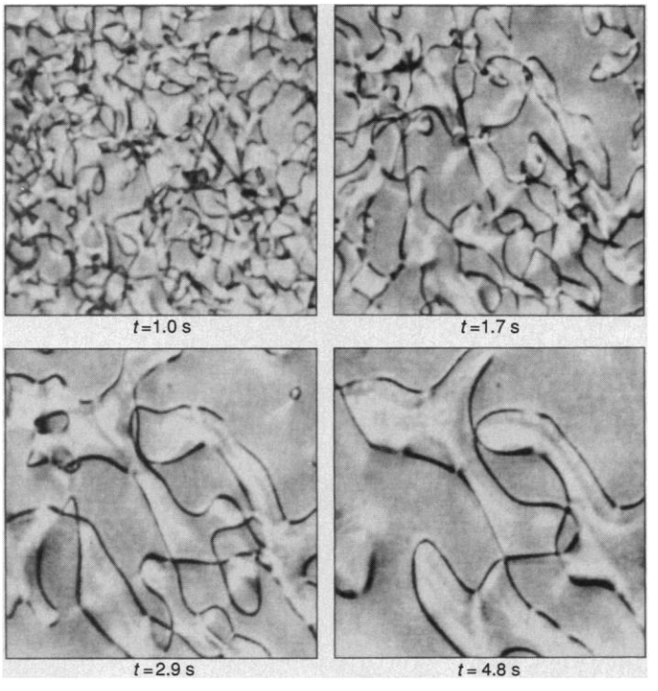

Fig. 4. A coarsening sequence showing the strings visible in our 230-μm-thick pressure cell containing K15 nematic liquid crystal, at $t = 1.0$, 1.7, 2.9, and 4.8 seconds after a pressure jump of $\Delta P = 4.7$ MPa from an initially isotropic state in equilibrium at approximately 33°C and 3.6 MPa. The evolution of the string network shows self-similar or "scaling" behavior. Each picture shows a region 360 μm in width.

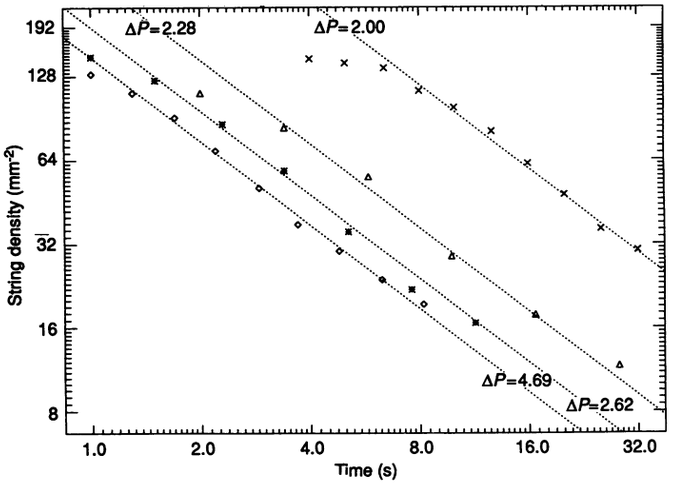

Fig. 5. String density data, accumulated at four different ΔP values. The scaling relation was experimentally determined to be $\xi \approx t^{0.51\pm0.04}$, where $\rho = 1/\xi^2$. For higher ΔP, the string tension is higher and one expects from the analysis in the text that the scaling density will be lower, which is observed.

and a detailed study of the scaling of the string density that supports both the Kibble mechanism and the one-scale model important in cosmology. We have also observed string intercommutation. However, there are many issues that remain to be explored. The defect tangle should be characterized in more detail. For example, the relative proportions of loops to long strings, $\pm\frac{1}{2}$ strings to ± 1 strings, and strings to monopoles should be determined. A systematic, microscopic description of the coarsening process would also be particularly useful. Certainly, further theoretical work is needed to explain the abundances of the various defects and their interaction rates. We hope that such work could eventually provide a more general framework for describing the evolution of cosmological defects.

REFERENCES AND NOTES

1. T. W. B. Kibble, *J. Phys. A* **9**, 1387 (1976).
2. A. Vilenkin, *Phys. Rep.* **9**, 1387 (1989).
3. N. Turok, *Phys. Rev. Lett.* **63**, 2625 (1989).
4. C. T. Hill, D. N. Schramm, J. N. Fry, *Comm. Nucl. Particle Phys.* **19**, 25 (1989).
5. W. H. Press, B. S. Ryden, D. N. Spergel, *Astrophys. J.* **347**, 590 (1989).
6. V. Kuzmin, V. Rubakov, M. Shaposhnikov, *Phys. Lett. B* **155**, 36 (1985).
7. M. Shaposhnikov, *Nucl. Phys. B* **287**, 757 (1987).
8. _____, *ibid.* **299**, 797 (1988).
9. N. Turok and J. Zadrozny, *Phys. Rev. Lett.* **65**, 2331 (1990).
10. J. D. Gunton, M. San Miguel, P. S. Sahni, in *Phase Transitions and Critical Phenomena*, C. Domb and J. L. Lebowitz, Eds. (Academic Press, New York, 1983), p. 267.
11. H. Furukawa, *Adv. Phys.* **34**, 703 (1985).
12. K. Kawasaki, *Phys. Rev. A* **31**, 3880 (1985).
13. H. Toyoki and K. Honda, *Prog. Theoret. Phys.* **78**, 237 (1987).
14. A. J. Bray, *Phys. Rev. Lett.* **62**, 2841 (1989).
15. M. Mondello and N. Goldenfeld, *Phys. Rev. A* **42**, 5865 (1990).
16. W. H. Zurek, *Nature* **317**, 505 (1985).
17. M. V. Kurik and O. D. Lavrentovich, *Sov. Phys. Usp.* **31**, 196 (1988).
18. G. Vertogen and W. H. de Jeu, *Thermotropic Liquid Crystals* (Springer-Verlag, Berlin, 1988).
19. P. G. de Gennes, *The Physics of Liquid Crystals* (Clarendon Press, Oxford, 1974).
20. D. Demus and L. Richter, *Textures of Liquid Crystals* (Verlag Chemie, New York, 1978).
21. Y. Bouligand, in *Les Houches Session XXXV, Physics of Defects*, R. Balian, Ed. (North-Holland, Dordrecht, 1981).
22. _____, *J. Phys.* **35**, 959 (1974).
23. _____, *ibid.* **34**, 1011 (1973).
24. T. Vachaspati and A. Vilenkin, *Phys. Rev. D* **30**, 2036 (1984).
25. D. Mitchell and N. Turok, *Phys. Rev. Lett.* **58**, 1577 (1987).
26. _____, *Nucl. Phys. B* **294**, 1138 (1987).
27. A. Albrecht and N. Turok, *Phys. Rev.* **40**, 973 (1989).
28. T. W. B. Kibble, *Nucl. Phys. B* **252**, 227 (1985).
29. M. Barriola and A. Vilenkin, *Phys. Rev. Lett.* **63**, 341 (1989).
30. N. Turok and D. Spergel, *ibid.* **64**, 2736 (1990).
31. D. Bennett and S. Rhie, *ibid.* **65**, 1709 (1990).
32. D. Spergel, N. Turok, W. Press, B. Ryden, *Phys. Rev. D*, in press.
33. A. Gooding, D. Spergel, N. Turok, *Astrophys. J.*, in press.
34. D. Spergel, C. Park, N. Turok, *ibid.*, in press.
35. It should be noted that the physically relevant "absolute" homotopy class is not exactly the same as mathematically defined "relative" homotopy class calculated here. This is important in the case of monopoles. For isolated monopoles, the absolute homotopy class in our case is just the positive integers (an "anti-monopole" is obtained from a monopole by reversing **n**, which of course changes nothing). However, two "monopoles" may be put together in such a way as to give a charge 2 object, or a charge 0 object. To calculate the topological properties of the combined system one needs to know how the monopoles are put together. For a discussion of this point and references, see appendix 2 in P. Goddard and D. Olive, *Rep. Prog. Phys.* **41**, 1357 (1978). This is often also called the influence of π_1 on π_2—one consequence is that a "monopole" can be made into an "antimonopole" by moving it around a string, as was discussed in G. E. Volovik and V. P. Mineev, *Sov. Phys. JETP* **45**, 561 (1976).
36. The symmetry group may equally well be taken to be O(3) broken to D_∞, but since the corresponding orbits are the same, $O(3)\mathbf{n} = SO(3)\mathbf{n}$, it is sufficient to consider SO(3) broken to O(2). This is of course also true for the tensor field.
37. P. P. Karat and N. V. Madhusudana, *Mol. Cryst. Liq. Cryst.* **40**, 239 (1977).
38. These are chosen by taking the δK_i to be functions of radius, which vanish outside some radius r. We do not fix the boundary conditions because that would prejudice the issue of which solution has minimal energy. However, perturbatively the result is very sensitive to boundary conditions, and if this behavior persists one would expect the monopoles in the liquid crystal to be rather variable too. For monopoles also, the saddle-splay contribution to the energy is important.
39. A. S. Goldhaber, *Phys. Rev. Lett.* **63**, 2158 (1989).
40. C. Williams, P. Pierański, P. E. Cladis, *ibid.* **29**, 90 (1972).
41. E. P. S. Shellard, *Nucl. Phys. B* **282**, 624 (1987).
42. R. Matzner, *Comput. Phys.* **2**, 51 (1988).
43. K. W. Schwarz, *Phys. Rev. D* **38**, 2398 (1988).
44. H. Nishimori and T. Nukii, *J. Phys. Soc. Jpn.* **58**, 563 (1988).
45. P. E. Cladis and M. Kléman, *J. Phys.* **33**, 591 (1972).
46. N. E. Steenrod, *The Topology of Fibre Bundles* (Princeton Univ. Press, Princeton, NJ, 1951).
47. G. H. Derrick, *J. Math. Phys.* **5**, 1252 (1964).
48. Y-S. Wu and A. Zee, *Nucl. Phys. B* **324**, 623 (1989).
49. It should be noted here that the string tension is not strictly a constant. In fact, in the one constant approximation it is given by $K\pi \ln(R/r_c)$ where r_c is the core radius and $R \approx \xi$ is the typical spacing between strings. However, one can also show using the "nematodynamic" (*19*) equations $\gamma\partial_t\mathbf{n} = -(\delta\mathcal{E}/\delta\mathbf{n})$ for a string moving at constant velocity v through the medium, that the damping force is also proportional to $\ln(R/r_c)$, so the above equations should hold even including this logarithmic correction.
50. I. M. Lifshitz and V. V. Slyosov, *J. Phys. Chem. Solids* **19**, 35 (1961).
51. D. P. Bennett and S. R. Bouchet, *Phys. Rev. Lett.* **63**, 2776 (1989).
52. B. Allen and E. P. S. Shellard, *ibid.* **64**, 119 (1990).
53. H. Orihara and Y. Ishibashi, *J. Phys. Soc. Jpn.* **55**, 2151 (1986).
54. H. Orihara, T. Nagaya, Y. Ishibashi, *ibid.* **56**, 3086 (1987).

55. N.T. acknowledges the support of NSF contract PHY80-19754. R.D. is supported in part by the Swiss National Science Foundation. We thank P. E. Cladis and M. Hindmarsh for stimulating and useful discussions.

5 November 1990; accepted 25 January 1991